Micro-structured electrode arrays: glow discharges in Ar at atmospheric pressure using a variable radio frequency generator

C. Schrader [1], L. Baars-Hibbe [1], E. M. van Veldhuizen [2], W. W. Stoffels [2], N. Lucas [3], P. Sichler [3], K.-H. Gericke [1], S. Büttgenbach [3]

[1]*Institut für Physikalische and Theoretische Chemie, Technische Universität Braunschweig, Hans-Sommer-Straße 10, D-38106 Braunschweig, Germany; E-Mail: K.Gericke@tu-bs.de*
[2]*Department of Physics, Technische Universiteit Eindhoven, Den Dolech 2, 5612 AZ Eindhoven, The Netherlands*
[3]*Institut für Mikrotechnik, Technische Universität Braunschweig, Alte Salzdahlumer Str. 20, D-38124 Braunschweig, Germany*

Micro-structured electrode (MSE) arrays consist of an interlocked, comb like, capacitive electrode system with gap widths in the µm-range. The usage of the Paschen similarity law (pd = const.) enabled us to generate large area uniform glow discharges up to atmospheric pressure with our arrays. In order to ignite glow discharges at atmospheric pressure this approach is established next to using dielectric barrier arrays and plasma jets. Because of the industrial, scientific and medical (ISM) limitation of available radio frequencies the usual frequency for experiments is 13.56 MHz. With a variable radio frequency generator, it is possible to extend the applicability of the MSE arrays in order to gain more information about the frequency dependent breakdown mechanisms and to confirm the underlying theory. The electric parameters of the non-thermal plasma system are characterized by a special probe with an upper frequency detection limit of 60 MHz.

1. Introduction

Non-thermal plasma processing at atmospheric pressure is the subject of growing interest due to the possible applications in plasma chemistry and excitation. There are many approaches published in the last 15 years to overcome the problems to generate and sustain stable, uniform and homogeneous non-thermal atmospheric pressure plasmas.

Massines et al. [1], Okazaki et al. [2], Trunec et al. [3] and Kelly-Wintenberg et al. [4] successfully generated atmospheric pressure glow discharges with a dielectric barrier array, and Park et al. [5] developed an atmospheric pressure plasma jet producing a stable and homogenous plasma. There are two approaches based on the Paschen similarity law ($p \cdot d$ = const.), which scale down the electrode dimensions to the micrometre range in order to ignite glow discharges at atmospheric pressure at moderate voltages working in the Paschen minima of the different gases.

Stark and Schoenbach [6], Penache et al. [7] and Eden et al. [8] use a micro-hollow-cathode array. We introduced micro-structured electrode arrays (MSE) consisting of an interlocked comb like electrode system with gap widths in the micrometre range [9-12]. The electrodes are arranged on an insulating substrate and are manufactured by means of modern micro-machining and galvanic techniques.

With the MSE array, it is possible to decompose perfluorocompounds (PFCs) [13]. CF_4 in particular is extensively used for semiconductor manufacturing processes, and as an exhaust gas of the processing tools it has proven to be particularly difficult to destroy and remove [14].

Another application of the MSE plasma source is the synergetic, successful concept of sterilisation and coating of food packaging materials. The reactive plasma species cause the physical destruction of the spores' cell walls, and induce the deposition of thin films as diffusion barrier resulting in packaging materials refinement [15]. In our sterilisation experiments the thermo resistant spores of the vegetative bacteria Bacillus cereus (B.cereus) and the UV resistant spores of the fungus Aspergillus niger (A. niger) were deactivated.

This publication presents a new step of realising a homogeneous atmospheric pressure plasma source with very low breakdown and burning voltages in nitrogen, oxygen and air, respectively. We show in argon at atmospheric pressure that we can control the breakdown mechanism and accordingly the breakdown voltages by varying the frequency.

2. Experimental

Figure 1 shows an MSE array and the electrode gap design supporting the ignition of the plasma. The design and production of the MSE arrays is already published in [13]. The characteristic MSE dimensions are electrode width (1350 µm), electrode thickness (100 µm) and electrode gap width (70 µm) in order to achieve high pressure ranges.
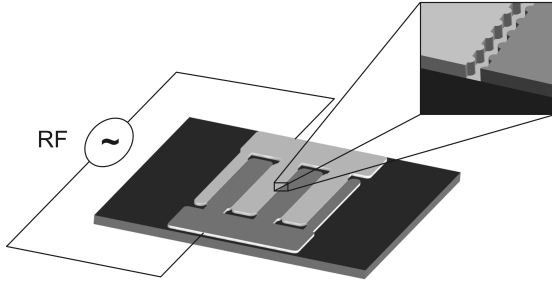

Fig. 1: Scheme of a micro-structured electrode (MSE) array.

The experimental setup in Figure 2 illustrates how the measurements with the special probe (ENI VI-Probe) with an upper frequency detection limit of 60 MHz have been carried out. The RF generator (Agilent 33250A 80 MHz connected to Amplifier Research Model 75AP250 75 W 5-250 MHz) is connected to the VI-Probe via a matching network (ENI MW-5D). A gas mixing unit supplies the vacuum chamber with different types of gases and the pressure control system adjusts the desired pressure.
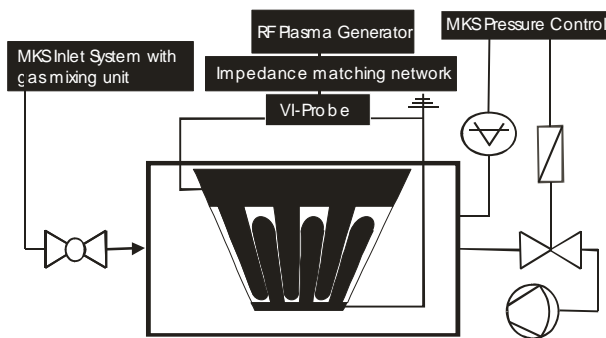

Fig. 2: Scheme of the experimental setup.

3. Characterization of the RF plasma

Due to the very small electrode gap width we can describe the behavior of the charged particles in the RF field of our system with the DC Townsend breakdown theory, depending on the pressure range and gas type.

In order to explain the observed breakdown behavior Fig. 3 shows the oscillation amplitudes z_0 of the Ar ions calculated with the measured electric field strength E_0 using equation (1)
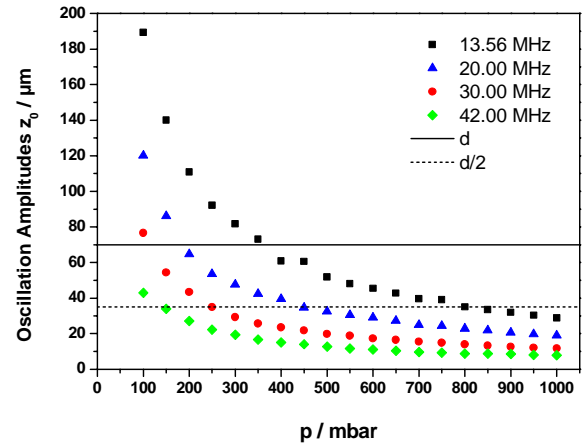

Fig. 3. Ar ion oscillation amplitudes for $d = 70$ µm calculated with the measured electric field strength.

$$z_0 = \frac{eE_0}{m\omega\sqrt{\omega^2 + v_C^2}} \qquad (1)$$

in which E_0 is the field amplitude, m the mass of the charged particle, ω the angular frequency and v_C the e⁻-neutral collision frequency. This equation gives the extreme values derived from the solution (3) of the equation of motion (2) including the pressure dependent Lorentz collisional term in order to account for friction [16].

$$m\frac{d^2z}{dt^2} + mv_c\frac{dz}{dt} = eE_0\sin\omega t \qquad (2)$$

$$z = -\frac{eE_0v_C}{m\omega(\omega^2 + v_C^2)}\cos(\omega t) - \frac{eE_0}{m(\omega^2 + v_C^2)}\sin(\omega t) \qquad (3)$$

The motion of the charged particle is drift controlled analogously to DC discharges, because the amplitudes of the electrons as well as the ions exceed $d/2$ (35 µm) [17]. Where the experimental curves resemble the Paschen curves they are fitted with the Paschen formula [18, 19] derived from the DC Townsend breakdown theory:

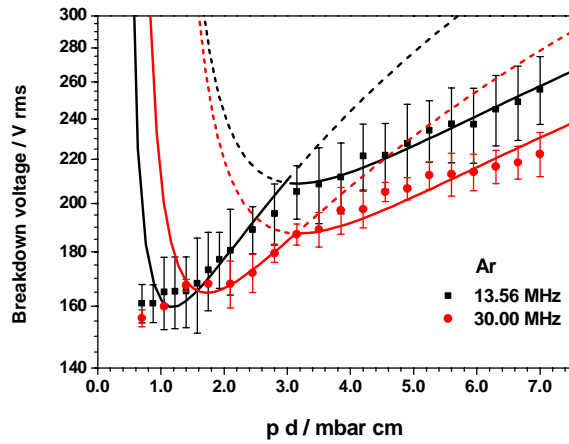$$U_{IP} = \frac{B(pd)}{C + \ln(pd)} \qquad (4)$$

Fig. 4. Fitted Paschen curves in Ar. Comparison of the breakdown voltages of the different frequencies. The curves of 20 MHz and 42 MHz are omitted for better clarity. The standard deviation describes the margin of deviation between three manufactured MSE samples.

with
$$C = \ln \frac{A}{\ln\left(\dfrac{1}{\gamma}+1\right)} \qquad (5)$$

The minima of the fitted curves exhibit the minimal ignition (breakdown) voltage. The maximum of equation (6)

$$\alpha = A \cdot p \cdot e^{-\left(\dfrac{B \cdot p}{E}\right)} \qquad (6)$$

corresponds to the minimal required voltage specified in equation (7).

The empiric constant B *(V mbar^{-1} cm^{-1})*, also known in this context as Stoljetow constant, is connected with the constant C from eqn. (4, 5) regarding the secondary electron amplification [20].

$$\left(\frac{E}{p}\right)_m = \left(\frac{U_{IP}}{p \cdot d}\right)_m = B \qquad (7)$$

The fitted constants B and C are listed in Table 1. The experimental secondary electron emission coefficients γ are calculated using equation (5) with $A = 9.0$ mbar^{-1} cm^{-1} [18]. For 13.56 MHz, the dominant breakdown mechanism changes from the DC Townsend mechanism (135.6 V mbar^{-1} cm^{-1}, γ regime,) at low pressures to the high frequency regime (66.2 V mbar^{-1} cm^{-1}, α regime) at high pressures [22]. Thus, the fit range is divided in two parts at the limit given by the DC region of applicability. The B values of the RF experiments determined for $d = 70$ µm are lower than the B values of the DC experiment [18] and decrease with increasing frequency. In the fit range at high pressures, where the high frequency mechanism already dominates at 13.56 MHz, the decrease of B with increasing frequency is not as strong as in the low pressure range. At low pressures, the dominating breakdown mechanism changes from the DC Townsend regime to the high frequency regime with increasing frequency. This interpretation is confirmed by Fig. 3: with increasing frequency the upper pressure limit fulfilling the $d/2$ criteria for the dominating DC Townsend regime ($z_0 > d/2$) is lowered, the high frequency regime becomes more dominant.

Table 1. Fitted constants of the Paschen formula and regions of applicability derived from Fig. 4 (B and E/p in V mbar^{-1} cm^{-1}) as well as the secondary electron emission coefficients γ calculated using equation (5).

Frequency	B	C	γ	E/p	Regime
DC	135 [17]	–	$3.4 \cdot 10^{-2}$ [21]	75 – 450	γ
13.56 MHz	66.2 ± 1.4	-0.15 ± 0.03	$2.88 \cdot 10^{-5}$	37 – 70	α
	135.6 ± 4.1	$+0.84 \pm 0.04$	$2.10 \cdot 10^{-2}$	70 – 184	γ
20.00 MHz	63.8 ± 2.4	-0.16 ± 0.05	$2.52 \cdot 10^{-5}$	34 – 72	α
	126.2 ± 2.3	$+0.73 \pm 0.03$	$1.31 \cdot 10^{-2}$	72 – 118	γ-α transition
30.00 MHz	58.9 ± 2.2	-0.16 ± 0.05	$2.52 \cdot 10^{-5}$	32 – 64	α
	95.4 ± 2.4	$+0.45 \pm 0.03$	$3.18 \cdot 10^{-3}$	64 – 120	γ-α transition
42.00 MHz	55.5 ± 0.9	-0.10 ± 0.02	$4.67 \cdot 10^{-5}$	30 – 58	α
	89.0 ± 3.7	$+0.48 \pm 0.05$	$3.77 \cdot 10^{-3}$	58 – 107	γ-α transition

The experimental γ values confirm the present results. With the transition of the breakdown mechanism at low pressures from 13.56 MHz to 30 MHz, the breakdown voltages increase slightly as shown in Figure 4 at low $p{\cdot}d$ values. The decreasing B value cannot compensate the strong decrease of the secondary electron emission coefficient γ (see Table 1) [22].

4. Ignition voltages dependent on applied radio frequencies

As already shown in Section 3 and demonstrated in He by Park et al [5], the breakdown voltages are dependent on the applied radio frequency. After the characterisation of our plasma source, we are able to predict that with the high frequency regime dominating the breakdown mechanism at atmospheric pressure the breakdown voltage decreases with increasing frequency as illustrated in Fig. 5. The standard deviation describes again the margin of deviation between three manufactured MSE samples.
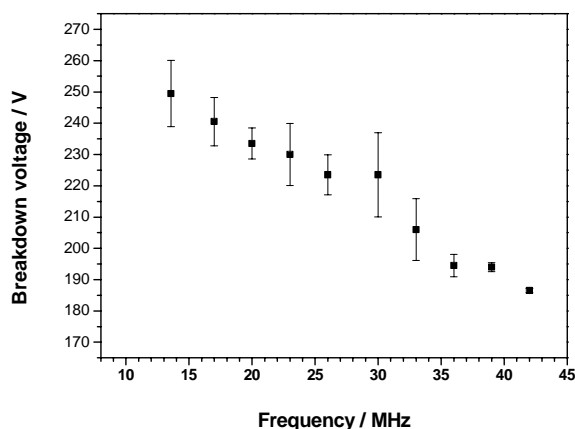

Fig. 5. Dependency of the experimental breakdown voltages on the applied frequency in 1000 mbar Ar.

Conclusions

This paper demonstrates a new promising path how the MSE arrays can be developed from a Paschen law optimized plasma source to an atmospheric pressure plasma application in several gases with discharge regime consideration. With variable RF frequencies it is possible to increase the working range and to improve the homogeneity of the plasma. Figure 5 demonstrates that further research in higher frequencies than 42 MHz may result in further improvement of the plasma generation process.

References

[1] F. Massines, A. Rabehi, P. Decomps, R. Ben Gadri, P. Ségur and C. Mayoux, J.Appl. Phys. **83** (1998) 2950-2957

[2] S. Okazaki, M. Kogoma, M. Uehara and Y. Kimura, J. Phys. D: Appl. Phys. **26** (1993) 889-892

[3] D. Trunec, A. Brablec and J. Buchte, J. Phys. D: Appl. Phys. **34** (2001) 1697-1699

[4] K. Kelly-Wintenberg, A. Hodge, T.C. Montie, L. Deleanu, D. Shermann, J. Reece Roth, P. Tsai and L. Wadsworth, J. Vac. Sci. Technol. **17** (1999) 1539-1544

[5] J. Park, I. Henins, H. W. Hermann and G. S. Selwyn, J. Appl. Phys. **89** (2001) 15-19

[6] R. H. Stark and K.H. Schoenbach, J. Appl. Phys. **85** (1999) 2075-2080

[7] C. Penache, A. Bräuning-Demian, L. Spielberger and H. Schmidt-Böcking, Proceedings of the Seventh International Symposium on High Pressure Low Temperature Plasma Chemistry (HAKONE VII), Greifswald (2000) 501-505

[8] J. G. Eden, S.-J. Park, N. P. Ostrom, S. T. McCain, C. J. Wagner, B. A. Vojak, J. Chen, C. Liu, P. von Allmen, F. Zenhausern, D. J. Sadler, C. Jensen, D. L. Wilcox and J. J. Ewing, J. Phys. D: Appl. Phys. **36** (2003) 2869-2877

[9] C. Geßner, P. Scheffler and K.-H. Gericke, Proc. of the Seventh International Symposium on High Pressure Low Temperature Plasma Chemistry (HAKONE VII), Greifswald (2000) 112-116

[10] C. Geßner, P. Scheffler and K.-H. Gericke, Proceed. of the International Conference on Phenomena in Ionized Gases (XXV ICPIG), Nagoya **4** (2001) 151-152

[11] H. Schlemm and D. Roth, Surf. Coat. Technol. **142-144** (2001) 272-276

[12] K.-H. Gericke, C. Geßner and P. Scheffler, Vacuum **65** (2002) 291-297

[13] L. Baars-Hibbe, P. Sichler, C. Schrader, C. Geßner, K.-H. Gericke and S. Büttgenbach, Surf. Coat. Technol. **174-175** (2003) 519-523

[14] C. Hartz, J. W. Bevan, M. W. Jackson, B. A. Wofford, Environ. Sci. Technol. **32** (1998) 682-687

[15] Final report of the research project: "Grundlagen zur Entkeimung und zur Diffusionssperre von nicht druckstabilen Hohlkörpern erzeugt mit Mikrowellenplasmen"; München (2004), Contract BMBF **13N7632,** Joint project no. **01016606**

[16] J. Reece Roth, Industrial Plasma Engineering, IOP Publishing, Bristol, Philadelphia (1995) 418-419

[17] K. Wiesemann, Einführung in die Gaselektronik, B.G. Teubner, Stuttgart (1976) 267-268

[18] Yu. P. Raizer, Gas Discharge Physics, Springer Verlag Berlin Heidelberg (1997) 56, 133-135

[19] A. Grill, Cold Plasma in Materials Fabrication IEEE Press, New York (1994) 24-34

[20] L. Baars-Hibbe, P. Sichler, C. Schrader, N. Lucas, K.-H. Gericke, S. Büttgenbach, J. Phys. D: Appl. Phys. **38** (2005) 510-517

[21] S. C. Brown, Basic Data of Plasma Physics, M.I.T. Press, Cambridge (1966), 219-235

[22] L. Baars-Hibbe, P. Sichler, C. Schrader, K.-H. Gericke, S. Büttgenbach, Plasma Process. Polym. **2** (2005) 174-182